

Detection of Cloud-Top Height from Backscattered Radiances within the Oxygen A Band. Part 2: Measurements

J. FISCHER AND W. CORDES

GKSS-Forschungszentrum, Geesthacht, Germany

A. SCHMITZ-PEIFFER, W. RENGER AND P. MÖRL

DLR, Wessling, Germany.

(Manuscript received 10 January 1990, in final form 20 January 1991)

ABSTRACT

Cloud-top heights were successfully derived from reflected solar radiation measurements within the oxygen A-band absorption. The accuracy of the estimated cloud-top heights was to within 40 meters over stratus clouds when compared with simultaneously taken lidar measurements. Estimations of the cloud optical thickness from reflected radiances at $\lambda = 755$ nm are reasonable. Between both cloud optical thickness and cloud-top height a positive cross correlation was found to be significant at scales up to 5 km, which confirms a relationship between cloud-top height and cloud optical thickness. These experimental results show the potential of multichannel radiance measurements for the detection of physical cloud properties.

1. Introduction

There are a few published experimental results dealing with remote sensing of physical cloud properties (Curran and Wu 1982; King et al. 1986, 1987; Foot 1988). One of the most important cloud properties with respect to global climate changes is cloud-top height and cloud optical thickness. Ohring and Adler (1978) postulate that an increase of 1 km in cloud height would result in a 1.2 K increase in surface temperature. Furthermore, a 1% change in cloud cover is estimated to have more than twice the effect of CO₂ doubling (Ramanathan et al. 1989). However, only global observations of cloud properties may serve global circulation model studies with sufficient input parameters so as to make them more realistic.

For the detection of cloud-top heights, we chose a method, based on reflected solar radiances within the O₂ A-band absorption centered at $\lambda = 761$ nm, that was first proposed by Yamamoto and Wark (1965) and discussed in Part 1 of this paper (Fischer and Grassl 1991). Following this theoretical study, the cloud-top height may be detected with an accuracy better than 200 m at a prescribed mean vertical profile of liquid-water content and for a cloud optical thickness $\delta_C > 5$. However, this investigation, which was based on radiative transfer calculations, did not include effects of all physical cloud properties, such as the three-dimen-

sional shape of clouds, which also determine the radiation field. Furthermore, the vertical profile of the cloud optical thickness affects the cloud-top height detection. However, all these properties affect the multispectral radiance measurements above clouds, and thus experimental data have to be used for a validation of such a cloud-top detection procedure.

Besides theoretical investigations, airborne measurements have shown that both cloud-top height and cloud optical thickness are detectable from multichannel measurements of the reflected solar radiation (Wu 1985; King 1987; Nakajima and King 1988). However, further aircraft measurements are necessary to study a wide variety of physical effects and to validate detection procedures derived from theoretical calculations. This is of particular interest with respect to forthcoming satellite sensors such as those proposed for the European Polar Platform (EPOP). These radiometers promise measurements of multispectral reflected solar radiation with a spectral resolution of a few nanometers, which implies new applications in the remote sensing of atmospheric properties (Fischer 1988).

For a first test and validation of a cloud-top height algorithm, such as that proposed by Fischer and Grassl (1991), we chose aircraft measurements from simultaneously operating lidar and optical multichannel analyzer sensors.

2. Instrumentation and algorithms

Before we discuss the experimental results, a short description of both instruments and the algorithms

Corresponding author address: Dr. Jürgen Fischer, Institut für Physik, GKSS-Forschungszentrum, Postfach 1160, 2054 Geesthacht, Germany.

used for the retrieval of cloud-top height and cloud optical thickness is given.

a. Multispectral radiance measurements

The multispectral radiances were measured with an optical multichannel analyzer (OMA), which is a commercial instrument manufactured by EG&G Princeton Applied Research. During the experiment the OMA was operated with a silicon photodiode array detector intensified by a microchannel plate (MCP). MCP intensifiers have sufficient sensitivity to detect less than 10 photoelectrons per digital count. However, clouds backscatter enough energy that microchannel plate intensifiers are not a prerequisite for the detection of physical cloud properties. However, the advantage of short exposure times is that they allow the high sampling frequency necessary for a high geometrical resolution of the radiance measurements. The spectral interval of each channel was set to about $\Delta\lambda \sim 0.6$ nm with a spectral region between $\lambda = 720$ and 780 nm. The control and data recording unit for the detector were manufactured at the GKSS research center. The receiver optic consists of a fiber cable and a photo telelense with $f = 300$ mm and an aperture of 4. This instrument configuration provide for a ground resolution of $\Delta x = 40$ m when flying at 10-km height.

The mean noise of the dark current of all channels was determined to within 0.5%. The radiance accuracy between the channels was found to be <1%, which was confirmed by the field measurements. The accuracy of the absolute radiances was < 7%.

The algorithms for the detection of cloud-top height and cloud optical thickness from multichannel radiance measurements were derived from radiative transfer calculations. The radiative transfer code used and the necessary input of optical properties are given in Fischer and Grassl (1991). This paper discusses explicitly the benefits of using radiance measurements within the O₂ absorption A band for the retrieval of cloud-top heights and proposes an algorithm for the estimation of cloud-top heights z_*^{top} from only two spectral radiance measurements:

$$Z_*^{\text{top}} = \frac{D}{R_{\text{Sat}}} + AR_{\text{Sat}} \left[B \frac{L_{\text{max}}}{L_{\text{Sat}}} + \exp\left(C \frac{L_{\text{max}}}{L_{\text{Sat}}}\right) \right]. \quad (1)$$

Parameter R_{Sat} is the ratio of the radiances measured at $\lambda = 755$ and 761 nm; L_{max} is the possible maximum upward radiance at $\lambda = 755$ nm reflected by clouds

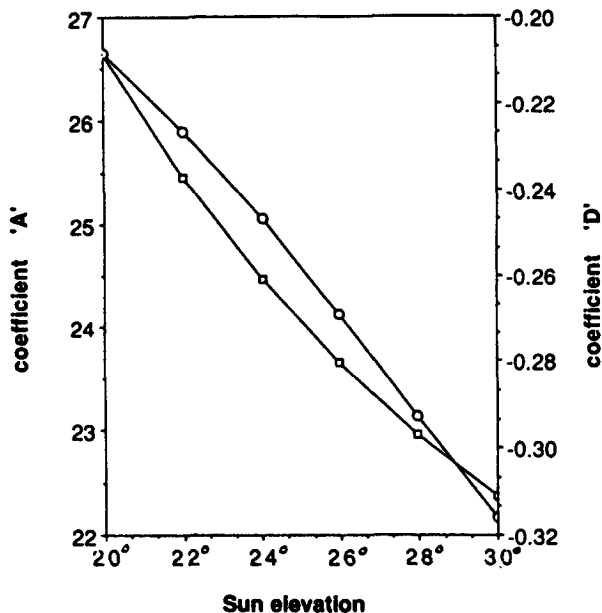


FIG. 1. Coefficients A (□) and D (○) of the cloud-top height algorithm [Eq. (1)] versus sun elevation θ_s .

and dependent on the solar zenith angle (Table 1); and L_{Sat} is the radiance that is actually measured at $\lambda = 755$ nm. The ratio $L_{\text{max}}/L_{\text{Sat}}$ provides information concerning the cloud optical thickness δ_C and thus enables us to correct for photon penetration effects. However, the coefficients A, B, C, and D, which were determined from radiative transfer calculations, were slightly redefined in order to take into account the conditions of this experiment. A midlatitude summer atmosphere is still assumed (McClatchey et al. 1972). Since the coefficients are sensitive to changes in solar elevation, as demonstrated in Fig. 1, even small time changes of 5 min have to be considered when estimating the mean cloud-top height to within an accuracy of ± 50 m. For the flight tracts O1–O4 of this experiment, we estimated the coefficients as given in Table 1.

The cloud optical thickness δ_C is simply derived from radiance measurements at $\lambda = 755$ nm. From radiative transfer calculations, we found a relationship between both quantities

$$\delta_C = 19.406 - 0.603 L_{\lambda=755 \text{ nm}} + 0.00584 L_{\lambda=755 \text{ nm}}^2 \quad (2)$$

TABLE 1. Theoretical maximum nadir radiance L_{max} ($\text{W m}^{-2} \text{sr}^{-1} \mu\text{m}^{-1}$), solar elevation θ_s , and coefficients A, B, C, and D of Eq. (1) used to estimate the cloud-top heights for the flight tracks O1–O4.

n	Time	θ_s	L_{max}	A	B	C	D
1	1555:30–1557:35	28.07°	176	22.914	0.0167	0.0	-0.2928
2	1559:30–1601:35	27.54°	179	23.083	0.0165	0.0	-0.2865
3	1604:30–1606:35	26.88°	182	23.310	0.0162	0.0	-0.2788
4	1609:30–1611:35	26.21°	185	23.554	0.0157	0.0	-0.2712

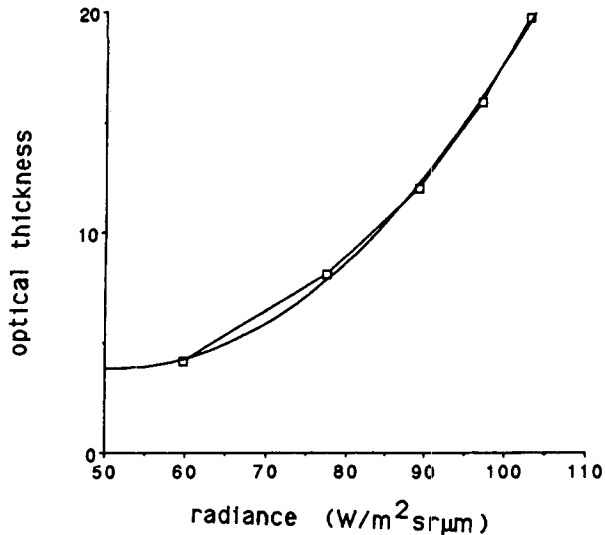


FIG. 2. Cloud optical thickness versus calculated radiances at $\lambda = 755$ nm. A stratus cloud with an effective radius of the cloud droplets of $r_{\text{eff}} = 5.25$ μm , a cloud-top height of $z^{\text{top}} = 1750$ m, a geometrical thickness of $\Delta z_c = 750$ m, and a sun elevation of $\theta_s = 30^\circ$ were assumed. The regression coefficient is $R = 0.998$.

which is illustrated in Fig. 2. This relationship was derived and is valid only for cloud optical thicknesses between $\delta_c = 5$ and $\delta_c = 30$ and a surface albedo of $\alpha = 0.2$. Uncertainties in the phase function of the cloud droplets can contribute to uncertainties in the derived optical thickness of 20% (King 1987). Since no microphysical cloud properties are measured during the experiment, further validation of cloud optical thickness estimates cannot be given.

b. Lidar measurements

The lidar measurements were performed using the backscatter lidar system ALEX-F onboard the meteorological research aircraft Falcon 20 of the DLR, Institute of Atmospheric Physics. Laser pulses at $\lambda = 1.06$ μm were emitted from the vertically downward-looking system through a window in the fuselage. The backscattered light, gathered by a telescope, is detected by a photodiode, amplified, digitized by a transient recorder, and finally stored on a computer compatible tape. For more details of the system used, see Mörl et al. (1981). Each laserpulse lasts 15 ns. The digitization rate is 50 MHz, which corresponds to a vertical resolution of 3 m. With a repetition rate of 3Hz, a maximum horizontal resolution of about 50 m is achieved.

The cloud-top height is derived from distance measurements from aircraft to cloud top. For the determination of the aircraft height, the recorded altimeter pressure data and the pressure and temperature profile of a midlatitude summer atmosphere were used (see McClatchey et al. 1972). However, the estimate of the aircraft altitude z^{air} depends on the atmospheric state: for a midlatitude summer atmosphere we derived z^{air}

= 9890 m, for a tropical atmosphere $z^{\text{air}} = 9929$ m, for a midlatitude winter atmosphere $z^{\text{air}} = 9248$ m, and for the actual atmosphere, measured during the ascent, $z^{\text{air}} = 9926$ m. Thus, uncertainties in atmospheric pressure and temperature profile result in uncertainties in cloud-top height estimates derived from lidar measurements.

The cloud extinction coefficient σ was derived from the decrease in the range corrected Lidar signal from 100% at the cloud top (z^{top}) to 80% within the cloud body ($z^{80\%}$).

$$\sigma = \frac{-\ln(0.8)}{2(z^{\text{top}} - z^{80\%})}. \quad (3)$$

For this altitude interval, the optical depth may be below 0.1, which implies that multiple scattering may be neglected for the receiver FOV of the used lidar. Therefore, we assume that σ is the single-scattering extinction coefficient. The mean penetration depth of the lidar signal is the range for which the lidar signal decreases to $1/e$ and was found to 48 m as a mean value during this experiment.

3. Flight experiment

The flight took place on the 21 September 1988 over southern Bavaria. At the eastern part of a high pressure system over western Europe, stratus cloud decks, typical for such weather conditions, covered a large area. The vertical extent of the cloud layer varied from 500 to 1000 m and cloud-top heights were between 1500 and 2000 m above sea level.

A Falcon jet was chosen as the measuring platform for both the optical multichannel analyzer and the lidar. The flight level during the experiment varied between 9000 and 10 000 m, the mean speed was around 160 m s^{-1} . During 55 min of flight time, a distance of 528 km was covered. Because of the limited storage capacity, each dataset of continuous OMA measurements represents a flight pattern of 20-km length.

4. Results

For a validation of cloud-top heights and cloud optical thickness derived from reflected solar radiation measurements, and because we used radiative transfer calculations to define the coefficients of the algorithm used for the estimation of cloud-top height and cloud optical thickness, we first compare calculated and measured multispectral radiances. A test of the cloud-top height algorithm [Eq. (1)] through a comparison of cloud-top heights derived from both OMA and lidar measurements is the main goal of this paper. In the last section we discuss the results for the cloud optical thickness.

a. Multispectral radiances

For a comparison of simulated and measured multispectral radiances in the O_2 A-band absorption centered

at $\lambda = 761$ nm, we chose radiance measurements along a 20-km flight leg, for which lidar measurements gave a mean cloud-top height $z^{\text{top}} = 1759$ m and a vertical cloud extent Δz_C of about 750 m. In Fig. 3a, the mean, minimum, and maximum values of upward radiances above a low-level stratus cloud layer are shown. All the main features of the upwelling radiation field due to the O_2 absorption, as predicted by radiative transfer modeling, were resolved. The spectral resolution was about $\Delta\lambda \sim 0.6$ nm. Calculated upward radiances over clouds with different cloud optical thicknesses but similar cloud-top height $z^{\text{top}} = 1750$ m are shown in Fig. 3b for $\Delta\lambda = 1.0$ nm. Both simulated and measured multispectral radiances behave almost identically, particularly within the O_2 absorption band. Measured and calculated multispectral radiances agree well, justifying

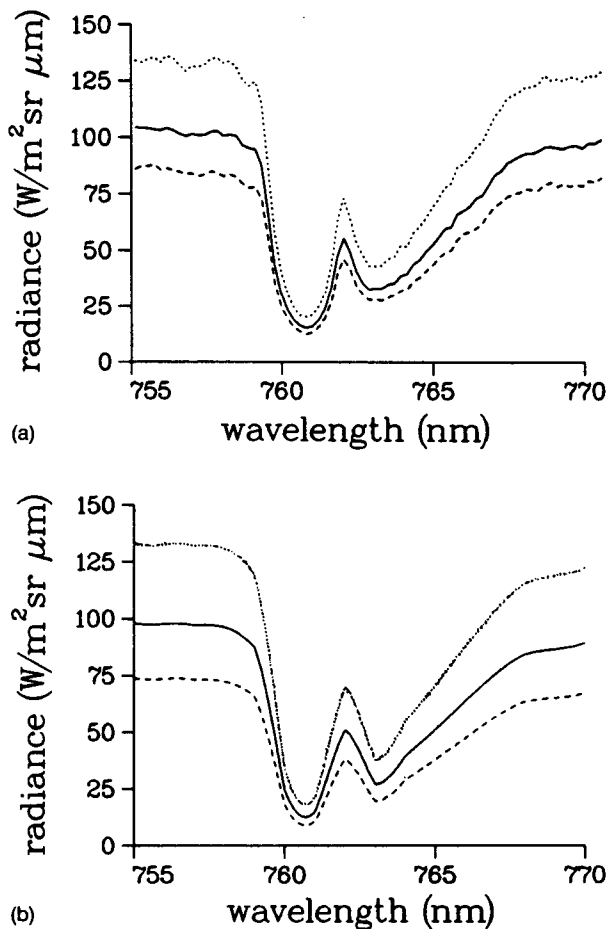


FIG. 3. (a) Upward spectral radiances measured from an aircraft (cruising altitude $z = 9.8$ km) above stratus clouds; the spectral resolution of the optical multichannel analyzer is about $\Delta\lambda = 0.6$ nm; the sun elevation is $\theta_S = 28^\circ$; lowest radiance (---), mean radiance (—), and highest radiance values (···) as found along a 20-km flight track. (b) Calculated upward spectral radiances at $z = 9.8$ km; the spectral resolution is $\Delta\lambda = 1.0$ nm; and the sun elevation is $\theta_S = 29^\circ$. For further cloud properties see Fig. 2. The assumed cloud optical thicknesses are $\delta_c = 4.2$ (---), $\delta_c = 8.1$ (—), and $\delta_c = 19.9$ (···).

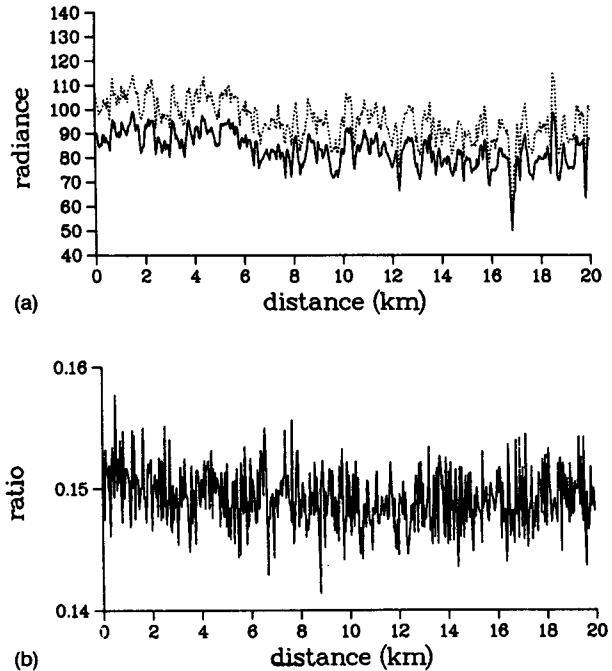


FIG. 4. (a) Measured upward radiances at $\lambda = 755$ (—) and 761 nm (···), the latter multiplied by 7.7; measurements obtained along flight track O2. (b) As in (a), but for the radiance ratio $L_{761 \text{ nm}} / L_{755 \text{ nm}}$.

the use of simulated radiances for the retrieval of an algorithm for cloud-top height detection.

b. Cloud-top height

The detection of cloud-top heights from reflected solar radiation is based on radiance measurements within and outside the O_2 A-band absorption. In Fig. 4a upward radiances at $\lambda = 755$ and 761 nm are shown along a 20-km flight track. The radiance values vary only by a factor of two. The radiance ratio shows quite large variations (Fig. 4b). Since this radiance ratio dominates the estimation of cloud-top heights using Eq. (1), we also find similar strong variations in cloud-top height well above cloud-top height changes derived from lidar measurements (Fig. 5). These differences are mainly due to the noise of the OMA measurements. As already mentioned in section 2, the relative radiance error was 0.5%, which leads to an over- or underestimation of cloud-top height of about 150 m.

If the signal-to-noise ratio of the OMA measurements is enhanced by sampling over ten single-measured radiances, which, of course, reduces the horizontal resolution to $\Delta x = 400$ m, the cloud-top heights derived from the OMA measurements agree better with those of the lidar measurements for all flight tracks analyzed (Figs. 6a–d). However, the OMA measurements still predict larger variations of cloud-top height, but the general features are resolved. Although both instruments could not be adjusted in this experiment

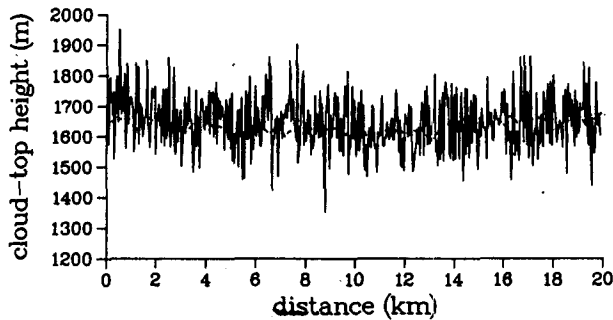


FIG. 5. Cloud-top heights derived from OMA (—) and lidar measurements (---) along flight track O2; the horizontal resolutions are $\Delta x = 40$ m for the OMA and $\Delta x = 130$ m for the lidar measurements. See also Fig. 4.

to look at identical cloud surfaces, we should expect similar features above the observed stratocumulus clouds. However, we also estimated statistical properties for a more detailed comparison. Both methods predict mean cloud-top heights, averaged over flight distances of 20 km, to within 40 m (Table 2). The standard deviations of all 4 flight tracks analyzed are of the same order of magnitude.

An estimation of the power spectra of both the OMA and lidar measurements gives some idea as to whether convective features can be resolved and further assists in the comparison of both cloud-top height detection methods. Former turbulence measurements confirm that the “energy” decreases with decreasing spatial scales within an inertial subrange where no energy production or dissipation takes place. For the inertial subrange, a $-5/3$ relationship between the square of the Fourier amplitudes and the frequency or wavenumber is established. We also find such a relationship for the cloud-top heights derived from both methods. The existence of a $-5/3$ fit suggests the presence of an inertial subrange for cloud-top height fluctuations. This was also found by Boers et al. (1988) for scales below 2 km.

The power spectrum of cloud-top heights derived from all single OMA measurements taken along four separate flight tracks with a total flight distance of 80 km results in a relationship of -0.67 . The “white noise” of the OMA measurements caused by instrumental noise is obvious for wavenumbers > 60 . For a cutoff wavenumber of 60, the power spectrum leads to a slope of -1.72 , a value that is very close to that found from previous measurements (Fig. 7a). Power spectra of cloud-top heights derived from both OMA and lidar measurements taken along identical flight tracks agree for wavenumbers < 40 (compare Figs. 7a,b). The agreement between both power spectra indicates that both cloud-top height retrieval methods work quite successfully. Since there is no physical explanation for the existence of a $-5/3$ fit for horizontal scales of cloud-top height variations > 2 km, we suggest that topo-

graphic effects are related to cloud height variations. According to these results, we conclude that cloud-top height fluctuations can be resolved with OMA measurements. However, more precise cloud-top heights may be derived, if the signal-to-noise ratio of the instrument is enhanced.

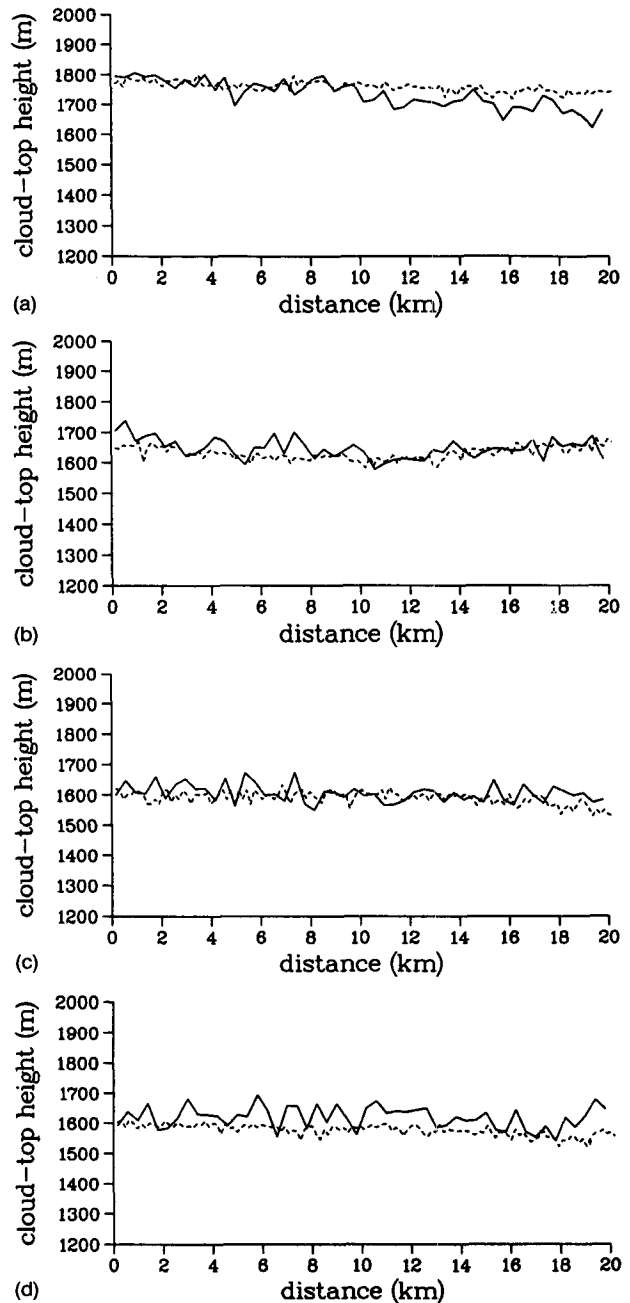
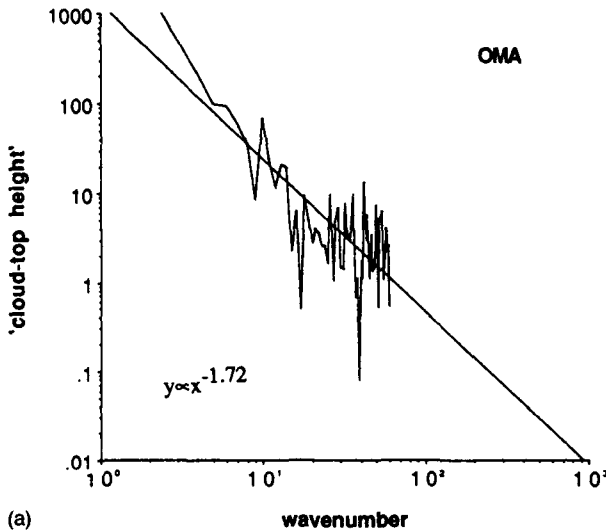


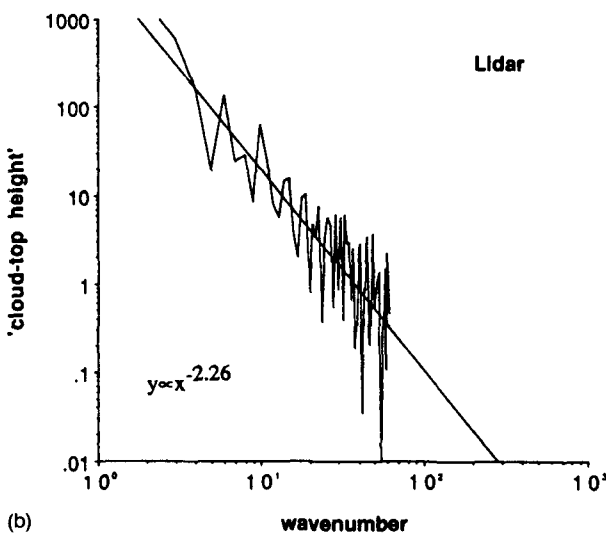
FIG. 6. (a) Cloud-top heights derived from OMA (—) and lidar measurements (---) along flight track O1; the OMA measurements are averaged over 10 samples, which results in a geometrical resolution of $\Delta x = 400$ m. See also Table 1. (b) As in (a), but for flight track O2. (c) As in (a), but for flight track O3. (d) As in (a), but for flight track O4.

TABLE 2. Mean (z_m^{top}) and standard deviation (z_s^{top}) of cloud-top heights for the flight tracks O1–O4.

n	Lidar		OMA	
	z_m^{top} (m)	z_s^{top} (m)	z_m^{top} (m)	z_s^{top} (m)
1	1759	16	1734	45
2	1632	21	1647	33
3	1589	22	1605	29
4	1576	19	1618	36



(a)



(b)

FIG. 7. (a) Spectral density of cloud-top height fluctuations relative to wavenumber $(80 \text{ km})^{-1}$, derived from OMA measurements O1–O4 (see Table 1); the overall flight distance amounts to 80 km and the spatial resolution is $\Delta x = 1333 \text{ m}$ relative to a cutoff wavenumber of 60. (b) Spectral density of cloud-top height fluctuations relative to wavenumber $(80 \text{ km})^{-1}$, derived from lidar measurements ($\Delta x = 130 \text{ m}$) of identical flight sections and also relative to a cutoff wavenumber of 60. The solid line is the regression curve.

c. Cloud optical thickness

The cloud optical thickness was derived from radiance measurements at $\lambda = 755 \text{ nm}$ using Eq. (2). For the analyzed flight track, the cloud optical thickness varied between $\delta_C = 8$ and $\delta_C = 18$ (Fig. 8). Although the instrumental noise does affect the radiance measurements and thus the retrieval of δ_C , estimates of δ_C without any averaging are reliable. Since additional microphysical cloud properties did not measure during the experiment, we are not able to verify the retrieval of the cloud optical thickness. We only estimated the cloud extinction coefficient from lidar measurements, which give some information about the upper layer of the clouds (see also Fig. 8).

The Fourier-transformed radiance measurements (Fig. 9a) and the Fourier-transformed cloud optical thickness (Fig. 9b) are comparable. The relationships between the square of the Fourier amplitudes and wavenumber are -1.75 and -1.79 , which also suggest an inertial subrange of convection. The estimates of the extinction coefficient derived from the lidar measurements lead to a slope of -0.62 (Fig. 9c).

The results of the OMA measurements suggest that both cloud-top height and cloud optical thickness are related to convective features of the stratus cloud. The comparison of the power spectra of both cloud optical thickness and extinction coefficient of the upper cloud layer indicates that the physical processes within and at the upper layer of the cloud are different. These may be convection within the cloud and radiative cooling at the top of the cloud.

The autocorrelation of z_C^{top} profiles indicate that z_C^{top} is significantly correlated at scales up to 2 km (Fig. 10b) and δ_C for scales up to 2.5 km (Fig. 10a). The positive cross correlation between both properties is also significant up to 2 km, which confirms a relationship between cloud-top height and cloud optical thickness (Fig. 10c). This result is in agreement with lidar measurements taken above Arctic stratus clouds, for which a correlation of cloud optical thickness and cloud-top height was also found (Finger et al. 1989).

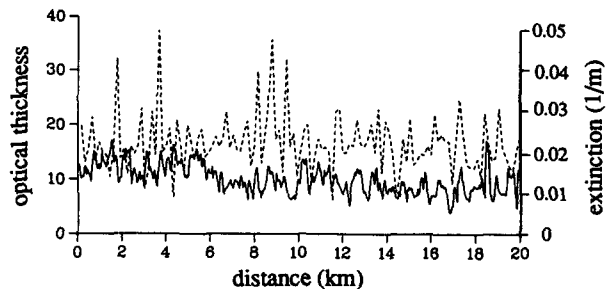


FIG. 8. Cloud optical thickness estimated from OMA (—) and extinction coefficients of the upper cloud layer derived from lidar measurements (---) along flight tract O2. See also Fig. 2.

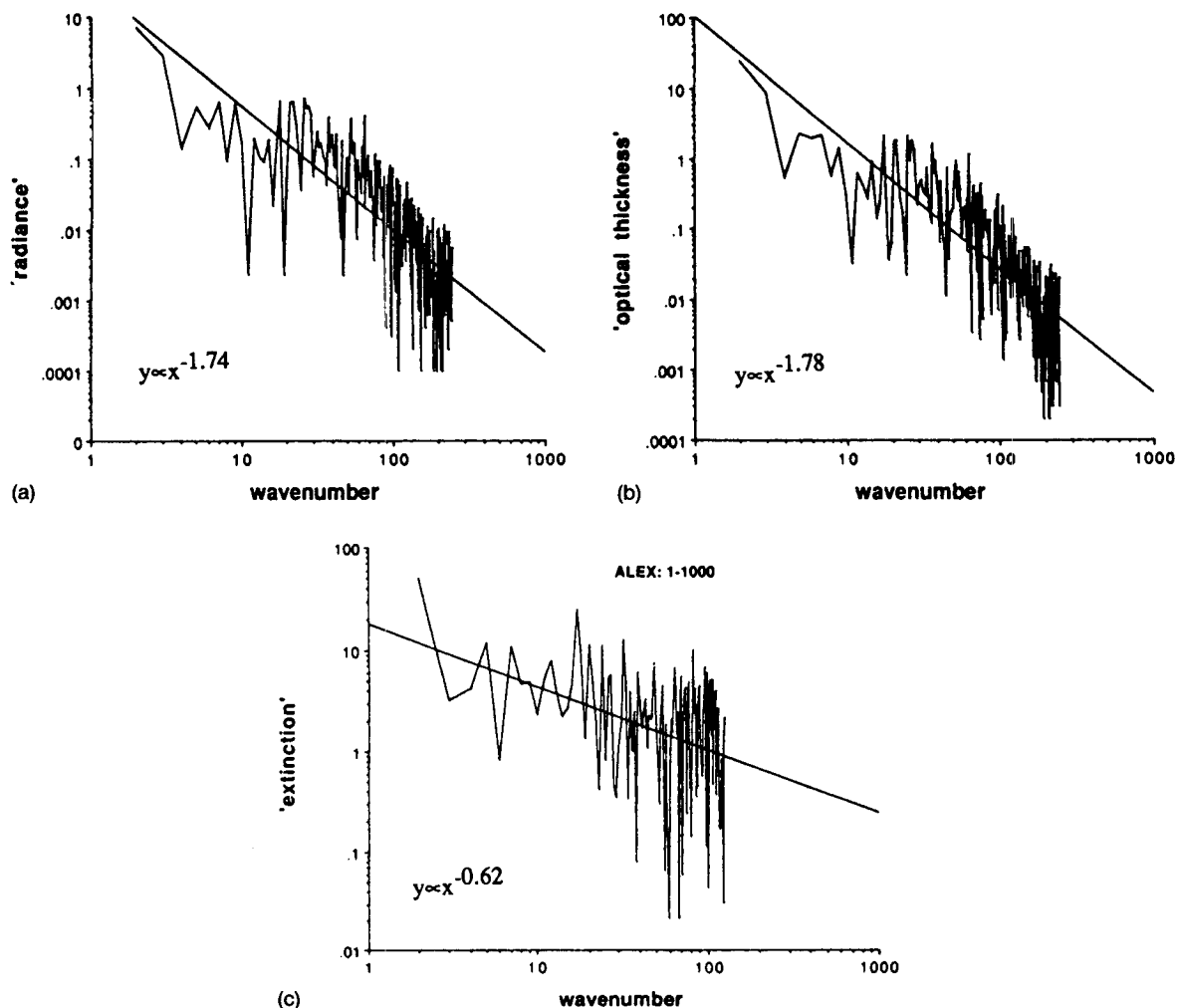


FIG. 9. (a) Spectral density of radiance fluctuations at $\lambda = 755$ nm relative to wavenumber $(80 \text{ km})^{-1}$, derived from OMA measurements O1–O4. See also Fig. 7(a). (b) As in (a), but for estimated cloud optical thickness. (c) Spectral density of fluctuations of the extinction coefficient relative to wavenumber $(80 \text{ km})^{-1}$ derived from lidar measurements.

5. Conclusions

Two methods have been presented for the determination of cloud-top height and the cloud optical thickness from reflected solar radiation measurements. A verification of both cloud properties derived from optical multichannel analyzer (OMA) measurements was tried by comparison with lidar measurements.

Cloud-top heights for a stratus deck were accurately predicted by the use of multichannel radiance measurements within the O_2 A-band absorption. Differences relative to lidar measurements were found to be less than 40 m. OMA measurements can also be used to resolve the convective structures of stratus clouds.

The horizontal structures and the extent of the cloud optical thickness derived from radiance measurements at $\lambda = 755$ nm are reasonable. The estimates of the

power spectra were used as a criterion for accurately predicting cloud optical thicknesses. Our findings are comparable to Boers et al. (1988), who found a similarity in the power spectra for the vertical velocity and radiance measurements at $\lambda = 754$ nm. All these results indicate that vertical velocity drives the cloud optical thickness and domes of cloud fields.

Measurements were performed only over low-level stratus clouds and thus our findings are valid only for such clouds. However, the fact that even small cloud-top height variations could be resolved with this method is encouraging enough to continue with further field experiments, which will have to take into account a greater variety of cloud types. Furthermore, the results of the radiative transfer calculations, such as presented in part 1 of this paper (Fischer and Grassl 1991), agree well for both multispectral radiances and predicted ac-

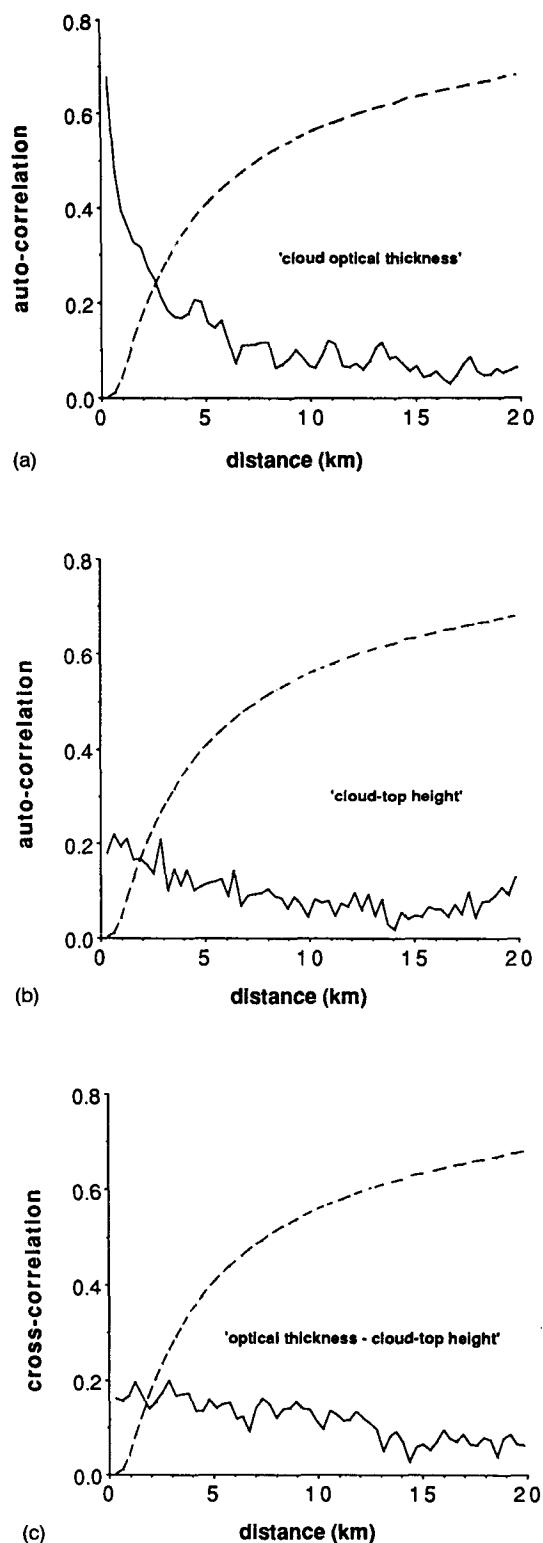


FIG. 10. (a) Autocorrelation of cloud-top height (—) along flight track O1–O4; the 95% significance level is indicated by (– –). (b) As in (a), but for cloud optical thickness. (c) Cross correlation of cloud-top height and cloud optical thickness as in (a).

curacy in cloud-top height detection. The anomalous absorption within the visible and near infrared, such as postulated by Twomey and Cocks (1982), was not found in our multispectral radiance measurements. However, during this experiment, the conditions were almost ideal in that the cloud decks were nearly horizontally homogeneous. Further experiments, taking into account various cloud types, are necessary in order to validate the inverse modeling technique as proposed in part 1. This approach is necessary when considering vertical variations in cloud optical thickness.

REFERENCES

- Boers, R., J. D. Spinhirne and W. D. Hart, 1988: Lidar observations of the fine-scale variability of marine stratocumulus clouds. *J. Appl. Meteor.*, **27**, 797–810.
- Curran, R. J., and M. L. Wu, 1982: Skylab near-infrared observations of clouds indicating supercooled liquid water droplets. *J. Atmos. Sci.*, **39**, 635–647.
- Finger, J., H. Förster, P. Mörl and A. Schmitz-Peiffer, 1989: Wellenphänomene an der Obergrenze von arktischen Stratuswolken, bestimmt aus Turbulenz-, Lidar- und Satellitenmessung. *Annalen der Meteorologie*, **26**, 187–188.
- Fischer, J., 1988: High resolution spectroscopy for remote sensing of physical cloud properties and water vapour. *Current Problems in Atmospheric Radiation*, Lenoble and Geleyn, Eds., Deepak, 151–154.
- , and H. Grassl, 1991: Detection of Cloud-top height from reflected radiances within the oxygen A band, Part 1: Theoretical studies. *J. Appl. Met.*, **30**, 1245–1259.
- Foot, J. S., 1988: Some observations of the optical properties of clouds. I: Stratocumulus. *Quart. J. Roy. Meteor. Soc.*, **114**, 129–144.
- King, M. D., 1987: Determination of scaled optical thickness of clouds from reflected solar radiation measurements. *J. Atmos. Sci.*, **44**, 1734–1751.
- , M. G. Strang, P. Leone and L. R. Blaine, 1986: Multiwavelength scanning radiometer for airborne measurements of scattered radiation within clouds. *J. Atmos. Ocean. Tech.*, **3**, 513–522.
- McClatchey, R. A., R. W. Fenn, J. A. Selby, F. E. Volz and J. S. Garing, 1972: Optical Properties of the atmosphere, AFRL-72.0497, Environmental Research Papers No. 411.
- Mörl, P., M. E. Reinhardt, W. Renger and R. Schellhase, 1981: The use of airborne lidar system ALEX-F for aerosol tracing in the lower troposphere. *Contr. Atm. Phys.*, **54**, 302–310.
- Nakajima, T., and M. D. King, 1988: Cloud optical parameters as derived from multispectral cloud radiometer. Vale, FIRE Science Experiment Team.
- Ohring, G., and S. Adler, 1978: Some experiments with a zonally averaged climate model. *J. Atmos. Sci.*, **35**, 186–205.
- Ramanathan, V., R. D. Cess, E. F. Harrison, P. Minnis, B. R. Barkstrom, E. Ahmad and D. Hartmann, 1989: Cloud-radiative forcing and climate: Results from the earth radiation budget experiment. *Science*, **243**, 57–63.
- Spinhirne, J. D., R. Boers and W. D. Hart, 1989: Cloud top liquid water from lidar observations of marine stratocumulus. *J. Appl. Meteor.*, **28**, 81–90.
- Twomey, S., and S. Cocks, 1982: Spectral reflectance of clouds in near-infrared: Comparison of measurements and calculations. *J. Met. Soc. Japan*, **60**, 583–592.
- Wu, M. L., 1985: Remote sensing of cloud-top pressure using reflected solar radiation in the oxygen A-band. *J. Clim. Appl. Meteor.*, **24**, 539–546.
- Yamamoto, G., and D. Q. Wark, 1961: Discussion of the letter by R. A. Hanel: Determination of cloud altitude from a satellite. *J. Geophys. Res.*, **66**, 3596.